

# Experimental entanglement quantification for unknown quantum states in a semi-device-independent manner

Yu GUO<sup>1,2,3</sup>, Lijinzhi LIN<sup>5</sup>, Huan CAO<sup>1,2,6</sup>, Chao ZHANG<sup>1,2</sup>, Xiaodie LIN<sup>5</sup>,  
Xiao-Min HU<sup>1,2</sup>, Bi-Heng LIU<sup>1,2\*</sup>, Yun-Feng HUANG<sup>1,2</sup>, Zhaohui WEI<sup>4,5\*</sup>,  
Yong-Jian HAN<sup>1,2\*</sup>, Chuan-Feng LI<sup>1,2\*</sup> & Guang-Can GUO<sup>1,2</sup>

<sup>1</sup>CAS Key Laboratory of Quantum Information, University of Science and Technology of China, Hefei 230026, China;

<sup>2</sup>CAS Center For Excellence in Quantum Information and Quantum Physics,  
University of Science and Technology of China, Hefei 230026, China;

<sup>3</sup>School of Physics and Materials Engineering, Hefei Normal University, Hefei 230601, China;

<sup>4</sup>Yau Mathematical Sciences Center, Tsinghua University, Beijing 100084, China;

<sup>5</sup>Center for Quantum Information, Institute for Interdisciplinary Information Sciences, Tsinghua University,  
Beijing 100084, China;

<sup>6</sup>Vienna Center for Quantum Science and Technology, Faculty of Physics, University of Vienna,  
Vienna A-1090, Austria

Received 9 September 2022/Revised 4 November 2022/Accepted 10 January 2023/Published online 4 July 2023

**Abstract** Using the concept of non-degenerate Bell inequality, we show that quantum entanglement, the critical resource for various quantum information processing tasks, can be quantified for any unknown quantum state in a semi-device-independent manner, where the quantification is based on the experimentally obtained probability distributions and prior knowledge of the quantum dimension only. Specifically, as an application of our approach to multi-level systems, we experimentally quantify the entanglement of formation and the entanglement of distillation for qutrit-qutrit quantum systems. In addition, to demonstrate our approach for multi-partite systems, we further quantify the geometric measure of entanglement of three-qubit quantum systems. Our results supply a general way to reliably quantify entanglement in multi-level and multi-partite systems, thus paving the way to characterize many-body quantum systems by quantifying the involved entanglement.

**Keywords** entanglement quantification, semi-device-independent, bell nonlocality, multi-partite system, multi-level system

**Citation** Guo Y, Lin L J Z, Cao H, et al. Experimental entanglement quantification for unknown quantum states in a semi-device-independent manner. *Sci China Inf Sci*, 2023, 66(8): 180506, <https://doi.org/10.1007/s11432-022-3681-2>

## 1 Introduction

Quantum entanglement, the key resource for quantum communication [1] and quantum key distribution [2–4], provides remarkable quantum advantages for quantum simulators and quantum computers over their classical counterparts [5, 6]. As a result, developing tools that can efficiently detect, or even quantify unknown quantum entanglement is a central problem in quantum information science. However, it is very challenging, as quantum entanglement cannot be measured directly by any observables.

To certify the existence of quantum entanglement, the concept of quantum entanglement witness [7] has been widely used. For an arbitrary entangled state  $\rho_{\text{ent}}$ , there is an entangled witness, defined as a Hermitian operator  $W$  such that for all separable states  $\text{Tr}(W\rho_{\text{sep}}) \geq 0$  but  $\text{Tr}(W\rho_{\text{ent}}) < 0$ . However, it is unsatisfactory for the following reasons: first, certain accurate information about the target state is needed [8], which prevents its application to unknown states; second, from the experimental aspect,

\* Corresponding author (email: bhliu@ustc.edu.cn, weizhaohui@gmail.com, smhan@ustc.edu.cn, cffi@ustc.edu.cn)

exact knowledge on the measurement devices needed by this approach is impossible to obtain; last, but not least, quantum entanglement witnesses usually only detect the presence of entanglement, which is insufficient for many applications such as classifying the topological phases in many-body systems by entanglement [9, 10].

The device-independent (DI) method, initially introduced in quantum key distribution [11] and self-testing [12], can also be used to detect the entanglement of a state. In this scenario, all the involved clients perform local measurements  $\{M_{\mathbf{x}}\}$  on the target quantum state and obtain corresponding outcomes  $\{\mathbf{a}\}$ , where  $\mathbf{x} \equiv (x_1, x_2, \dots, x_n)$  and  $\mathbf{a} \equiv (a_1, a_2, \dots, a_n)$  are the collections of the labels for measurement settings and outcomes. Then entanglement can be detected based only on the violation of a Bell-type inequality  $I(\rho, \{M_{\mathbf{x}}\}, \{\mathbf{a}\}) = \sum_{\mathbf{a}, \mathbf{x}} c_{\mathbf{x}}^{\mathbf{a}} p(\mathbf{a}|\mathbf{x}) \leq C_l$  ( $c_{\mathbf{x}}^{\mathbf{a}}$  are real coefficients and  $C_l$  is the classical bound). As a result, this approach can overcome the critical drawbacks of the entanglement witness method mentioned above. In fact, the DI method has been experimentally implemented to demonstrate dimension witness [13, 14], Bell-inequality violation [15], randomness generation [16], and self-testing [17]. Furthermore, measurement-DI [18, 19] and semi-DI schemes [20, 21], where partial information on the target system is known reliably, have also been extensively studied. For example, semi-DI schemes assume that the quantum dimension is known reliably before characterizing the target unknown quantum system.

Compared with entanglement detection, the quantification of entanglement is much more challenging. Particularly, when the full information of target quantum states is known, some important measures, such as the entanglement of formation and the entanglement of distillation, have been proposed to quantify bipartite quantum entanglement [22, 23]. Similarly, although with much more complicated mathematical structures, a few measures that can quantify multi-partite quantum entanglement have also been utilized, which include the geometric measure of entanglement (GME) and the relative entropy of entanglement [23–26]. Meanwhile, quantifying unknown quantum entanglement in that the underlying density matrices are not available is also a realistic problem, which is even harder as one has to characterize target quantum states first.

In this paper, we experimentally demonstrate that the semi-DI method can be utilized to efficiently quantify unknown entanglement in multi-level and many-body quantum systems. Particularly, since the foundation of our method is Bell-type correlations, whose size is not determined by the quantum dimension directly, the number of quantum measurements needed is very modest, implying that our method is very efficient.

More specifically, with the help of the Collins-Gisin-Linden-Masser-Popescu (CGLMP) inequality [27], we quantify the entanglement of formation and the entanglement of distillation in qutrit-qutrit systems based only on the experimentally obtained probability distributions, demonstrating our approach on multi-level systems. In addition, as a demonstration of multi-partite entanglement quantification, we further quantify the geometric measure of entanglement in 3-qubit systems by examining experimentally obtained probability distributions with the Mermin-Ardehali-Belinskii-Klyshko (MABK) inequality [28–30]. Although our experiments are performed on qutrit-qutrit bipartite quantum systems and 3-qubit quantum systems, we would like to stress that the semi-DI approach we demonstrated works generally for multi-level and many-body systems of arbitrary size, thus paving the way to studying many-body quantum systems by efficiently quantifying their entanglement.

## 2 Theoretical derivation of the semi-DI entanglement measure

We consider the entanglement quantification scenario in which an  $n$ -partite quantum state is distributed to  $n$  distant clients. For each experimental trial, the  $i$ th client performs a choice of measurement setting on his shared subsystems upon receiving a classical random input  $x_i$  and obtains a classical output  $a_i$ . After repeating the experiment sufficiently many times and collecting the observed statistics, the clients can generate a quantum correlation expressed as the probability distribution  $p(\mathbf{a}|\mathbf{x}) = \text{Tr}((\bigotimes_{i=1}^n M_{x_i}^{a_i})\rho)$ , where  $M_{x_i}^{a_i}$  is the measurement operator with outcome  $a_i$  for the measurement  $x_i$  performed on the  $i$ -th party. For convenience, let  $\{M_{\mathbf{x}}\}$  denote the tensor product of all local measurements  $\bigotimes_{i=1}^n M_{x_i}^{a_i}$ . The probability distribution  $p(\mathbf{a}|\mathbf{x})$  can then be used to detect nonlocality. Here, we further use them to quantify the entanglement of unknown quantum states of known dimension, that is, in a semi-DI fashion.

To quantify the entanglement of a multi-partite quantum state, a general measure is needed and we choose the GME [24, 25, 31]. The GME of a general quantum state  $\rho$  is defined by convex roof construction

as

$$E_G(\rho) \equiv 1 - \max_{\rho = \sum_i p_i |\psi_i\rangle\langle\psi_i|} \sum_i p_i \sup_{|\phi_i\rangle \in \text{sep}_n} |\langle\psi_i|\phi_i\rangle|^2,$$

where  $\text{sep}_n$  is the set of  $n$ -partite product pure states.

To obtain the GME from  $p(\mathbf{a}|\mathbf{x})$ , we need to calculate two fundamental quantities. The first is the maximal overlap between  $\rho$  and a pure product state  $|\phi\rangle$ , denoted by  $\hat{F}$ . Using the properties of quantum measurements,  $\hat{F}$  can be directly computed by numerical approaches such as the shifted higher-order power method (SHOPM) algorithm [32] from the distribution  $p(\mathbf{a}|\mathbf{x})$  [33] (see Supplemental Material for more details). Meanwhile, if  $\rho$  is pure, it is not hard to see that the GME is exactly  $1 - \hat{F}^2$ . However, for the general case that  $\rho$  is not pure, this relation does not hold. To address the general case, we need to estimate the second quantity, the purity of  $\rho$  (it means how it is close to a pure state, defined as  $\text{Tr}(\rho^2)$ ). The basic idea is as follows: if somehow we can prove that the purity of  $\rho$  is high, some term in the orthogonal decomposition of  $\rho$  has a large weight, which means that this term is a pure state that is very close to  $\rho$ . As a pure state, it is relatively easy to estimate its GME, then by utilizing the continuity of the GME, we can eventually estimate the GME of  $\rho$  (see Ref. [33] for more details on how this idea works).

Fortunately, if one applies the concept of non-degenerate Bell inequalities [34], a lower bound for the purity of  $\rho$  can be obtained directly from the distribution  $p(\mathbf{a}|\mathbf{x})$ . Supposing a set of local measurements and the corresponding outcomes have been labeled as  $(\{M_{\mathbf{x}}\})$  and  $(\{\mathbf{a}\})$ , respectively, a general Bell inequality can be expressed as  $I(\rho, \{M_{\mathbf{x}}\}, \{\mathbf{a}\}) = \sum_{\mathbf{a}, \mathbf{x}} c_{\mathbf{x}}^{\mathbf{a}} p(\mathbf{a}|\mathbf{x}) \leq C_l$ , where  $c_{\mathbf{x}}^{\mathbf{a}}$  are real numbers and  $C_l$  is the maximal classical value. Intuitively, if a quantum state  $\rho$  remarkably violates the Bell inequality  $I(\rho, \{M_{\mathbf{x}}\}, \{\mathbf{a}\}) \leq C_l$ , we hope  $\rho$  can be certified to be close to a pure state; i.e., the purity  $\text{Tr}(\rho^2)$  is close to 1, as in the Clauser-Horne-Shimony-Holt (CHSH) inequality [35]. The concept of non-degenerate for Bell inequalities is used to make this intuition strict. Explicitly, supposing the target quantum system has a dimension vector  $\mathbf{d} \equiv (d_1, d_2, \dots, d_n)$  (i.e.,  $d_i$  is the dimension of the  $i$ -th party),  $I(\rho, \{M_{\mathbf{x}}\}, \{\mathbf{a}\}) \leq C_l$  is called non-degenerate if there exist two real numbers  $0 \leq \epsilon_1 < \epsilon_2 \leq C_q(\mathbf{d})$  ( $C_q(\mathbf{d})$  is the maximal value of the Bell expression for quantum systems of given dimension vector  $\mathbf{d}$ ) such that, for any two orthogonal quantum states  $|\alpha\rangle$  and  $|\beta\rangle$ ,  $I(|\alpha\rangle\langle\alpha|, \{M_{\mathbf{x}}\}, \{\mathbf{a}\}) \geq C_q(\mathbf{d}) - \epsilon_1$  always implies that  $I(|\beta\rangle\langle\beta|, \{M_{\mathbf{x}}\}, \{\mathbf{a}\}) \leq C_q(\mathbf{d}) - \epsilon_2$ . In fact, many notable Bell inequalities, such as the MABK inequality in qubit systems and the CGLMP inequality in qutrit systems, have been proven to be non-degenerate [33, 34, 36].

Supposing the Bell inequality  $I(\rho, \{M_{\mathbf{x}}\}, \{\mathbf{a}\}) \leq C_l$  is non-degenerate with parameters  $\epsilon_1$  and  $\epsilon_2$ ,  $\rho$  has an orthogonal decomposition  $\rho = \sum_i a_i |\psi_i\rangle\langle\psi_i|$ , and  $I(\rho, \{M_{\mathbf{x}}\}, \{\mathbf{a}\}) \geq C_q(\mathbf{d}) - \epsilon_1$ . Then, according to the definition of the non-degenerate, it can be proven that there exists  $a_i$  such that  $a_i \geq 1 - \epsilon_1/\epsilon_2$  (without loss of generality, we suppose  $i = 1$ ; see Supplemental Material for more details) [33]. Particularly, when  $I(|\alpha\rangle\langle\alpha|, \{M_{\mathbf{x}}\}, \{\mathbf{a}\})$  is very close to  $C_q$ , it turns out that  $\epsilon_1$  and  $\epsilon_2$  can be chosen such that  $\epsilon_1/\epsilon_2 \ll 1$ , implying that  $\rho$  is close to a pure state [34], which is consistent with the intuition mentioned above.

With the estimations for  $\hat{F}$  and  $a_1$ , as mentioned above we are ready to apply the continuous property of the GME. If  $\hat{F} \leq a_1$ , a lower bound for the GME of  $\rho$  can be obtained as [33]

$$E_G(\rho) \geq \max_{c \in [\frac{\hat{F}}{\sqrt{a_1}}, \sqrt{a_1}]} \frac{a_1 - c^2}{1 - c^2} \left( 1 - \left( \frac{\hat{F}}{\sqrt{a_1}} c + \sqrt{1 - \frac{\hat{F}^2}{a_1}} \sqrt{1 - c^2} \right)^2 \right).$$

Actually, in addition to the GME, one can also lower bound the relative entropy of entanglement (REE)  $E_R(\rho)$  for  $\rho$  [23] by estimating  $a_1$  and  $\hat{F}$ . Indeed, with the technique introduced in [37], the information on  $a_1$  allows us to upper bound  $S(\rho)$ , the von Neumann entropy of  $\rho$  that plays a key role in many-body systems [38]. Combining this result with the information on  $\hat{F}$ ,  $E_R(\rho)$  can be directly lower bounded using the relation  $E_R(\rho) \geq -2 \log_2(\hat{F}) - S(\rho)$  [39].

Specifically, if  $\rho$  is restricted to a  $d \times d$ -dimensional bipartite quantum state, the entanglement of formation (denoted by  $E_f(\rho)$ ) [22] and the entanglement of distillation (denoted by  $E_d(\rho)$ ) [22] can also be quantified in a semi-DI manner. For this, first note that both entanglement measures can be lower bounded by the coherent information of  $\rho$ , defined by  $I_C(\rho) = S(\rho_A) - S(\rho)$  [40, 41], i.e.,  $E_f(\rho) \geq E_d(\rho) \geq I_C(\rho)$  [42]. Furthermore, the coherent information  $I_C(\rho)$  can be lower bounded by upper bounding  $S(\rho)$  and lower bounding  $S(\rho_A)$  simultaneously from the correlation data  $p(a_1 a_2 | x_1 x_2)$  (the dimension  $d$  of the bipartite system is known) [34]. As a result, the entanglement of formation and distillation can be lower bounded semi-device-independently.

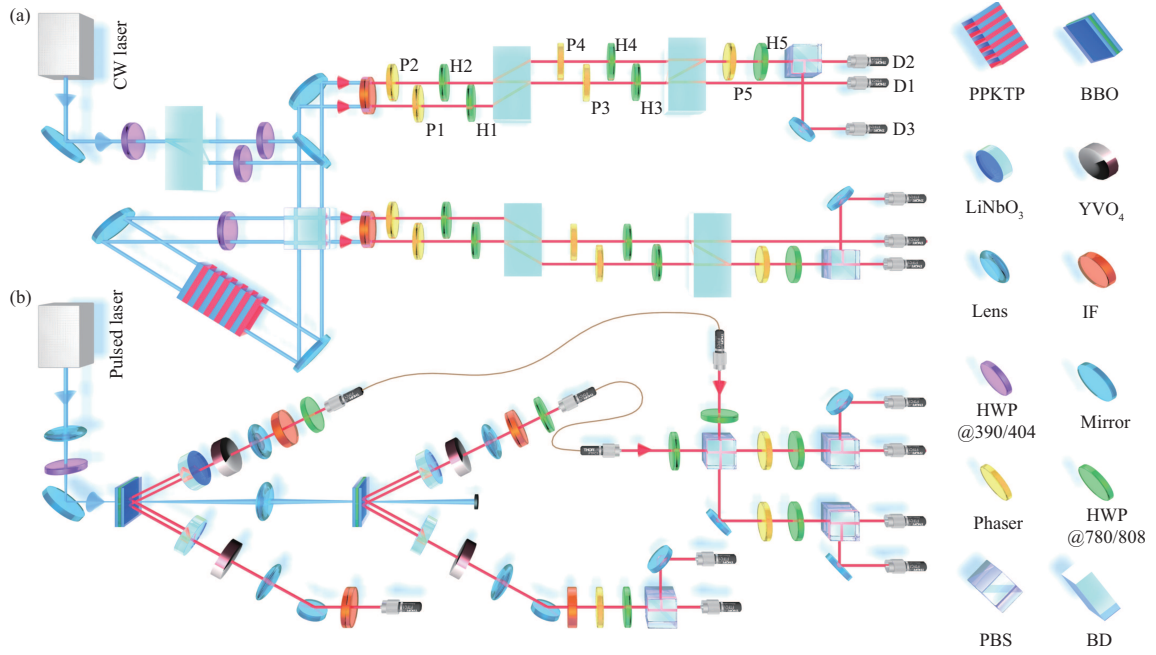


**Figure 1** (Color online) Experimental setup for the semi-DI entanglement quantification of (a) qutrit-qutrit and (b) three-qubit entangled states, both of which can be decomposed into an entangled source and a measurement apparatus. (a) An entangled photon pair is generated from SPDC at a type-II cut periodically poled KTP (PPKTP) crystal embedded in a two-path Sagnac interferometer and pumped by a continuous-wave (CW) violet laser (power is 4 mW, working at 404 nm). Qutrit-qutrit states are encoded in the hybrid of the path and polarization degrees of freedom of the photons. The measurement settings for the CGLMP inequality can be implemented via the configuration composed of a series of Phasers (a combination of two QWPs and an HWP), HWPs, BDs, and PBS. (b) Polarization-encoded three-photon GHZ states are produced by combining two pairs of entangled photons generated from two sandwich-like BBO crystals pumped by an ultraviolet laser (with a central wavelength of 390 nm, a pulse repetition rate of 80 MHz, and a power of 25 mW). LiNbO<sub>3</sub> and YVO<sub>4</sub> are used for spatial and temporal compensations between horizontal and vertical polarizations, respectively. IF: interference filter; HWP: half-wave plate; QWP: quarter-wave plate; PBS: polarizing beam splitter; BD: beam displacer.

### 3 Experimental implementation and results

#### 3.1 Experimental setups

The experimental setup to implement the semi-DI entanglement quantification for multi-level and multi-partite quantum states is shown in Figure 1. The setup mainly consists of entangled photon sources and measurement simulations for corresponding non-degenerate Bell-type inequalities.

In Figure 1(a), we use a high-quality path-polarization hybrid encoded entanglement source [43] to generate desired entangled states beyond the qubit state space. In particular, two-qutrit states of the form  $|\Phi(\beta)\rangle = (|00\rangle + \beta|11\rangle + |22\rangle)/\sqrt{2 + \beta^2}$  with varied  $\beta$  are prepared by means of the process of degenerate spontaneous parametric down-conversion (SPDC). Here, the vertically polarized (V) photon in the upper path is encoded as state  $|0\rangle$ , and the horizontally polarized (H) and vertically polarized photons in the lower path are encoded as state  $|1\rangle$  and  $|2\rangle$ , respectively. The real coefficient  $\beta$  is controlled by varying the angles of the half-wave plates (HWPs) at 404 nm. In Figure 1(b), two ultra-bright beamlike EPR photon sources are used to generate the 3-partite Greenberger-Horne-Zeilinger (GHZ) state  $|\Psi\rangle_3 = (|HHH\rangle + i|VVV\rangle)/\sqrt{2}$  [44]. Here an HOM-interferometer ensures photons from different EPR sources are indistinguishable in arrival time, frequency, and spatial degree of freedom, and the post-selection on two events  $|HHHH\rangle$  and  $|VVVV\rangle$  results in a 4-photon GHZ state. The desired state  $|\Psi\rangle_3$  can be obtained when one of the photons acts as a trigger and a phaser properly adjusts the relative phase between  $|HHH\rangle$  and  $|VVV\rangle$ .

#### 3.2 Entanglement of qutrit-qutrit states

The previously introduced semi-DI entanglement quantification method is general and can be applied to any multi-level and multi-partite states. We first apply it on a  $3 \times 3$  quantum system. Here both Alice and Bob are required to randomly perform two measurements on their qutrits to test a Bell-type

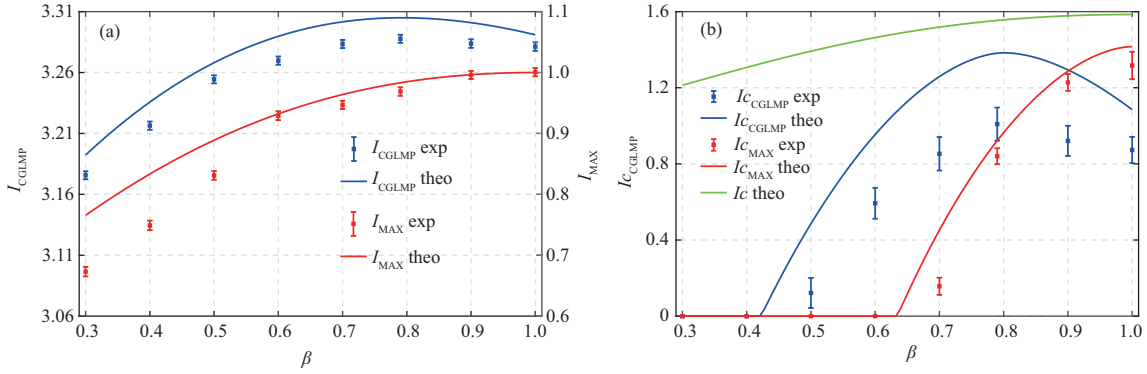


**Figure 2** (Color online) Results of semi-DI entanglement quantification for qutrit-qutrit states, where  $\beta \in [0.3, 1]$ . (a) Experimentally observed Bell expressions of the CGLMP inequality  $I_{\text{CGLMP}}$  and the inequality tailored for maximally entangled state  $I_{\text{MAX}}$  are marked as blue and red dots, respectively, while the theoretical predictions are plotted in blue and red lines. (b) Coherent information  $I_{\text{C}}$  as a lower bound for the entanglement measures of the state  $|\Phi(\beta)\rangle$ . Experimental results are marked as blue and red dots for the two inequalities, respectively, and the theoretical predictions using our method are plotted in the blue and red lines. For comparison, we also plot the exact coherent information of perfect  $|\Phi(\beta)\rangle$  as the green line.

inequality. If we choose the inequality to be the 3-dimensional CGLMP inequality (or the Bell inequality tailored to maximally entangled states [45], see Supplemental Material for details [46, 47]), the involved four measurements have projection states admitting a general quantum-mechanical formula as

$$\begin{aligned}
 |o(0)\rangle &= \frac{1}{\sqrt{3}}(|0\rangle + e^{i\alpha_1}|1\rangle + e^{i\alpha_2}|2\rangle), \\
 |o(1)\rangle &= \frac{1}{\sqrt{3}}(|0\rangle + e^{i(\alpha_1+2\pi/3)}|1\rangle + e^{i(\alpha_2+4\pi/3)}|2\rangle), \\
 |o(2)\rangle &= \frac{1}{\sqrt{3}}(|0\rangle + e^{i(\alpha_1+4\pi/3)}|1\rangle + e^{i(\alpha_2+8\pi/3)}|2\rangle),
 \end{aligned}$$

where the phases  $\alpha_1, \alpha_2 \in [0, 2\pi)$ . As depicted in Figure 1(a), the above measurements can be realized by placing five phasers (P), five HWPs, two beam displacers (BDs), a polarizing beam splitter (PBS), and three single photon detectors sequentially. Specifically, P2, P3 and P5 are set at  $\alpha_1 - \alpha_2$ ,  $-\alpha_1$ , and  $-(\alpha_1 + \pi/2)$ , and HWP1-5 are rotated at  $45^\circ$ ,  $67.5^\circ$ ,  $72.37^\circ$ ,  $45^\circ$ , and  $22.5^\circ$ . P1 and P4 set at 0 are used for temporal compensation, and detectors D1–D3 record three outcomes 0–2, respectively. Here the phaser consisting of two quarter-wave plates (QWPs) and an HWP can add an arbitrary phase between the H and V components.

As the first demonstration, we report our experimental results on the two bipartite Bell expressions in Figure 2, where the values of Bell expressions can be seen in Figure 2(a) and the lower bound for the coherent information can be seen in Figure 2(b). Here the class of states we chose is  $|\Phi(\beta)\rangle$  with  $\beta \in [0.3, 1]$ . As mentioned before, coherent information is a lower bound for the entanglement of formation and the entanglement of distillation. In Figure 2, our experimental data are marked with colored points, while the theoretical predictions (produce quantum correlations using perfect quantum states and measurements, then apply our method if needed) are given as colored solid lines. Specifically, the blue points and line represent results for the CGLMP inequality, and the red points and line are for the inequality tailored for maximally entangled states introduced in [45]. For comparison, we also plot the exact value of the coherent information as a green solid line in Figure 2(b). It can be seen that the measured Bell expressions match well with the theoretical lines, implying high-precision preparations and measurements of the qutrit-qutrit states. When choosing the CGLMP inequality, we obtain maximal coherent information of  $I_{\text{C}} = 1.01 \pm 0.09$  for  $\beta = 0.79$ , which coincides with the trend of theoretical prediction. Additionally, the minimal  $\beta$  in our experiment that we can set to certify entanglement is 0.5, while theoretically the coherent information should be positive when  $\beta$  is larger than  $\beta_{\text{min}} = 0.4223$ . See the Supplemental Material for experimental results or more details on  $a_1$  and  $\hat{F}$ .

A blemish of the CGLMP inequality when used as an entanglement quantifier is that the maximal violation is not obtained by the maximally entangled state. This can be avoided by utilizing the inequality tailored for maximally entangled states (see Supplemental Material section for details). With this inequality, the detected coherent information increases with the parameter  $\beta$ , and a maximum of

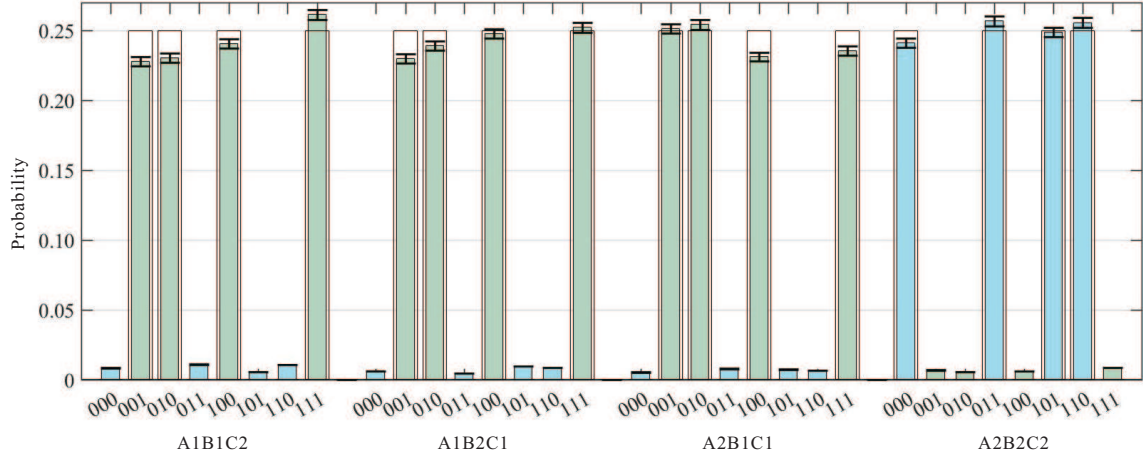


**Figure 3** (Color online) Results on semi-DI entanglement quantification for the 3-qubit GHZ state. To test the 3-partite MABK inequality, Alice, Bob, and Charlie randomly perform Pauli X or Pauli Y measurements on their qubits. The colored bars are the experimentally observed probabilities that obtain different outcomes on different measurement settings, with the corresponding theoretical predictions shown in grey edges. ‘A1B1C2’ means Alice and Bob perform Pauli X and Charlie performs Pauli Y measurement, and ‘001’ means their outcomes are  $-1, -1, 1$ , respectively. Light green and light blue bars represent that the number of outcome 1 is odd and even, respectively. From these statistics, we obtain a value of the MABK expression  $I_{\text{MABK}} = 1.895 \pm 0.013$  and a corresponding lower bound for the GME  $E_G(|\Psi\rangle_3) \geq 0.169 \pm 0.006$ .

$I_C = 1.32 \pm 0.07$  is obtained for maximally entangled qutrits, indicating a highly visible signal of entanglement beyond qubit systems. As a cost, the region of detectable states narrows down to approximately  $\beta \geq 0.64$ , which is verified in our experiment, and we successfully observe the existence of entanglement at  $\beta = 0.7$ .

### 3.3 GME of the 3-qubit GHZ state

Then, we apply the method to quantify the entanglement of a multi-partite system. We test the 3-partite MABK inequality (see Supplemental Material for details) on a 3-photon GHZ state  $|\Psi\rangle_3$ , where Alice, Bob, and Charlie randomly choose one of two Pauli measurements (Pauli X and Pauli Y) on their qubits. Single-qubit Pauli measurements can be achieved by an assemblage of a phaser, an HWP, and a PBS. The measured statistics are recorded and later used to calculate the corresponding MABK expression, which allows us to lower bound the entanglement of the underlying quantum state. As shown in Figure 3, we list the measured statistics in colored bars. From these correlations, we obtain an MABK inequality expression value of  $I_{\text{MABK}} = 1.895 \pm 0.013$  and a GME of  $E_G(|\Psi\rangle_3) = 0.169 \pm 0.006$ , while the theoretical predictions are 2 and 0.5, respectively. Here, despite these mismatches, our results show the enormous potential of non-degenerate Bell inequalities in quantifying multi-partite entanglement. The error bars of all the data are calculated from 100 simulations of Poisson statistics.

## 4 Conclusion

We have demonstrated semi-DI multi-level and multi-partite entanglement quantification in a proof-of-principle experiment by preparing a class of entangled photonic qutrits and tripartite photonic GHZ states. Despite the detection loophole, our result, together with existing measurement-DI scenarios [18, 19, 48, 49], marks an important step towards complete DI entanglement quantification of quantum systems. Because of the generality of the method, it potentially provides us with the opportunity to obtain critical information about many-body quantum physics, such as thermalization [50, 51], many-body localization [51, 52], and topological order [9, 10, 53].

**Acknowledgements** This work was supported by National Key Research and Development Program of China (Grant No. 2021YFE0113100), National Natural Science Foundation of China (Grant Nos. 11821404, 11904357, 12204458, 61832015, 62272259), Fundamental Research Funds for the Central Universities, China Postdoctoral Science Foundation (Grant No. 2021M700138), China Postdoctoral for Innovative Talents (Grant No. BX2021289), USTC Tang Scholarship, and Science and Technological Fund of Anhui Province for Outstanding Youth (Grant No. 2008085J02). This work was partially carried out at the USTC Center for Micro and Nanoscale Research and Fabrication.

**Supporting information** See Supplemental Material for details about the quantities  $a_1$ ,  $\hat{F}$ , and the Bell-type inequalities used in this work, including Refs. [46, 47]. The supporting information is available online at [info.scichina.com](http://info.scichina.com) and [link.springer.com](http://link.springer.com). The supporting materials are published as submitted, without typesetting or editing. The responsibility for scientific accuracy and content remains entirely with the authors.

## References

- 1 Gisin N, Thew R. Quantum communication. *Nat Photon*, 2007, 1: 165–171
- 2 Bennett C H, Brassard G. Quantum cryptography: public key distribution and coin tossing. *Theoretical Comput Sci*, 2014, 560: 7–11
- 3 Ekert A K. Quantum cryptography based on Bell's theorem. *Phys Rev Lett*, 1991, 67: 661–663
- 4 Gisin N, Ribordy G, Tittel W, et al. Quantum cryptography. *Rev Mod Phys*, 2002, 74: 145–195
- 5 Raussendorf R, Briegel H J. A one-way quantum computer. *Phys Rev Lett*, 2001, 86: 5188–5191
- 6 Vidal G. Efficient classical simulation of slightly entangled quantum computations. *Phys Rev Lett*, 2003, 91: 147902
- 7 Gühne O, Tóth G. Entanglement detection. *Phys Rep*, 2009, 474: 1–75
- 8 Rosset D, Ferretti-Schöbitz R, Bancal J D, et al. Imperfect measurement settings: implications for quantum state tomography and entanglement witnesses. *Phys Rev A*, 2012, 86: 062325
- 9 Levin M, Wen X G. Detecting topological order in a ground state wave function. *Phys Rev Lett*, 2006, 96: 110405
- 10 Kitaev A, Preskill J. Topological entanglement entropy. *Phys Rev Lett*, 2006, 96: 110404
- 11 Acín A, Brunner N, Gisin N, et al. Device-independent security of quantum cryptography against collective attacks. *Phys Rev Lett*, 2007, 98: 230501
- 12 Mayers D, Yao A. Self testing quantum apparatus. *Quantum Inf Comput*, 2004, 4: 273–286
- 13 Ahrens J, Badziąg P, Cabello A, et al. Experimental device-independent tests of classical and quantum dimensions. *Nat Phys*, 2012, 8: 592–595
- 14 Hendrych M, Gallego R, Mićuda M, et al. Experimental estimation of the dimension of classical and quantum systems. *Nat Phys*, 2012, 8: 588–591
- 15 Hensen B, Bernien H, Dréau A E, et al. Loophole-free Bell inequality violation using electron spins separated by 1.3 kilometres. *Nature*, 2015, 526: 682–686
- 16 Liu Y, Zhao Q, Li M H, et al. Device-independent quantum random-number generation. *Nature*, 2018, 562: 548–551
- 17 Zhang W H, Chen G, Peng X X, et al. Experimental realization of robust self-testing of bell state measurements. *Phys Rev Lett*, 2019, 122: 090402
- 18 Lo H K, Curty M, Qi B. Measurement-device-independent quantum key distribution. *Phys Rev Lett*, 2012, 108: 130503
- 19 Braunstein S L, Pirandola S. Side-channel-free quantum key distribution. *Phys Rev Lett*, 2012, 108: 130502
- 20 Moroder T, Gittsovich O. Calibration-robust entanglement detection beyond Bell inequalities. *Phys Rev A*, 2012, 85: 032301
- 21 Liang Y C, Vértesi T, Brunner N. Semi-device-independent bounds on entanglement. *Phys Rev A*, 2011, 83: 022108
- 22 Bennett C H, Divincenzo D P, Smolin J A, et al. Mixed-state entanglement and quantum error correction. *Phys Rev A*, 1996, 54: 3824–3851
- 23 Vedral V, Plenio M B, Rippin M A, et al. Quantifying entanglement. *Phys Rev Lett*, 1997, 78: 2275–2279
- 24 Brody D C, Hughston L P. Geometric quantum mechanics. *J Geometry Phys*, 2001, 38: 19–53
- 25 Wei T C, Goldbart P M. Geometric measure of entanglement and applications to bipartite and multipartite quantum states. *Phys Rev A*, 2003, 68: 042307
- 26 Vedral V, Plenio M B. Entanglement measures and purification procedures. *Phys Rev A*, 1998, 57: 1619–1633
- 27 Collins D, Gisin N, Popescu S, et al. Bell-type inequalities to detect true-body nonseparability. *Phys Rev Lett*, 2002, 88: 170405
- 28 Mermin N D. Extreme quantum entanglement in a superposition of macroscopically distinct states. *Phys Rev Lett*, 1990, 65: 1838–1840
- 29 Ardehali M. Bell inequalities with a magnitude of violation that grows exponentially with the number of particles. *Phys Rev A*, 1992, 46: 5375–5378
- 30 Belinskii A V, Klyshko D N. Interference of light and Bell's theorem. *Physics-Uspekhi*, 1993, 36: 653–693
- 31 Dai Y, Dong Y, Xu Z, et al. Experimentally accessible lower bounds for genuine multipartite entanglement and coherence measures. *Phys Rev Appl*, 2020, 13: 054022
- 32 Kolda T G, Mayo J R. Shifted power method for computing tensor eigenpairs. *SIAM J Matrix Anal Appl*, 2011, 32: 1095–1124
- 33 Lin L, Wei Z. Quantifying multipartite quantum entanglement in a semi-device-independent manner. *Phys Rev A*, 2021, 104: 062433
- 34 Wei Z, Lin L. Analytic semi-device-independent entanglement quantification for bipartite quantum states. *Phys Rev A*, 2021, 103: 032215
- 35 Clauser J F, Horne M A, Shimony A, et al. Proposed experiment to test local hidden variable theories. *Phys Rev Lett*, 1970, 24: 549
- 36 Scarani V, Gisin N. Spectral decomposition of Bell's operators for qubits. *J Phys A-Math Gen*, 2001, 34: 6043–6053
- 37 Smith G, Smolin J A, Yuan X, et al. Quantifying coherence and entanglement via simple measurements. 2017. ArXiv: 1707.09928
- 38 Nielsen M A, Chuang I L. *Quantum Computation and Quantum Information*. Cambridge: Cambridge University Press, 2000
- 39 Wei T C. Relative entropy of entanglement for multipartite mixed states: Permutation-invariant states and Dür states. *Phys Rev A*, 2008, 78: 012327
- 40 Schumacher B, Nielsen M A. Quantum data processing and error correction. *Phys Rev A*, 1996, 54: 2629–2635
- 41 Lloyd S. Capacity of the noisy quantum channel. *Phys Rev A*, 1997, 55: 1613–1622
- 42 Cornelio M F, de Oliveira M C, Fanchini F F. Entanglement irreversibility from quantum discord and quantum deficit. *Phys Rev Lett*, 2011, 107: 020502
- 43 Hu X M, Guo Y, Liu B H, et al. Beating the channel capacity limit for superdense coding with entangled ququarts. *Sci Adv*, 2018, 4: eaat9304
- 44 Zhang C, Huang Y F, Zhang C J, et al. Generation and applications of an ultrahigh-fidelity four-photon Greenberger-Horne-Zeilinger state. *Opt Express*, 2016, 24: 27059
- 45 Salavrakos A, Augusiak R, Tura J, et al. Bell inequalities tailored to maximally entangled states. *Phys Rev Lett*, 2017, 119: 040402
- 46 Ragnarsson S, van Loan C F. Block tensors and symmetric embeddings. *Linear Algebra its Appl*, 2013, 438: 853–874

- 47 Zohren S, Gill R D. Maximal violation of the Collins-Gisin-Linden-Massar-Popescu inequality for infinite dimensional states. *Phys Rev Lett*, 2008, 100: 120406
- 48 Guo Y, Cheng S, Hu X, et al. Experimental measurement-device-independent quantum steering and randomness generation beyond qubits. *Phys Rev Lett*, 2019, 123: 170402
- 49 Guo Y, Yu B C, Hu X M, et al. Measurement-device-independent quantification of irreducible high-dimensional entanglement. *npj Quantum Inf*, 2020, 6: 52
- 50 Srednicki M. Chaos and quantum thermalization. *Phys Rev E*, 1994, 50: 888–901
- 51 Abanin D A, Altman E, Bloch I, et al. Colloquium: many-body localization, thermalization, and entanglement. *Rev Mod Phys*, 2019, 91: 021001
- 52 Schreiber M, Hodgman S S, Bordia P, et al. Observation of many-body localization of interacting fermions in a quasirandom optical lattice. *Science*, 2015, 349: 842–845
- 53 Wen X G. Topological orders and edge excitations in fractional quantum Hall states. *Adv Phys*, 1995, 44: 405–473